Aalto University
School of Science
and Technology

PHYS-E0562 Nuclear Engineering, advanced course
Lecture 8 – Full-core calculations and nodal diffusion method

Jaakko Leppänen (Lecturer), Ville Valtavirta (Assistant)

Department of Applied Physics
Aalto University, School of Science
Jaakko.Leppanen@vtt.fi

May 9, 2018

Topics of this

Diffusion theory revisited

- Approximations and validity
- Two-group diffusion calculations
- Spatial homogenization

Full-core calculations:

- Global and local heterogeneous and homogeneous flux
- Discontinuity factors and equivalence theory
- Nodal diffusion method
- Pin-power reconstruction

Parametrization of group constants:

- Branch and history variations
- Fission product poisons

Example of homogenization and core simulation

Diffusion theory revisited

As pointed out in the previous lecture, solution to the global transport problem is obtained by dividing the calculation task into several parts.

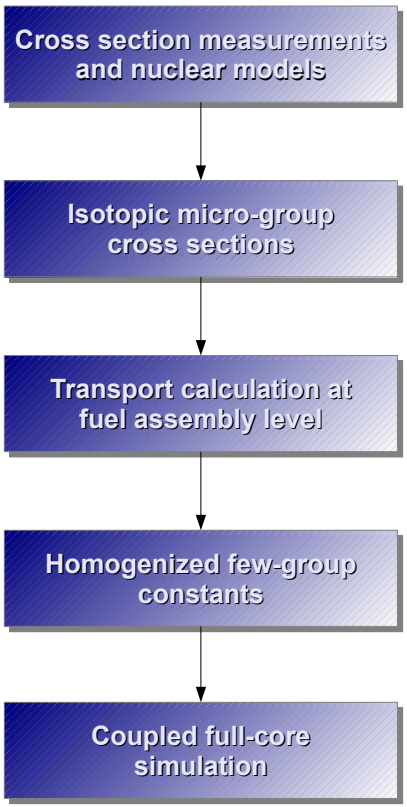

The spatial scale of the modeled system is gradually increased, while simultaneously moving towards more simplified description of physics

Local reaction rate balance is preserved at each step, by calculating flux-volume averaged cross sections based on the solution to the local transport problem

A major part of the complicated interaction physics is included already in the multi-group cross sections used in assembly-level calculations, for example:

- Doppler-broadening of cross sections
- Corrections for spatial and resonance self-shielding

All information on microscopic reaction rates, including their spatial distribution, is lost when the interaction physics is condensed into a handful of few-group constants.

Spatial homogenization not only enables running the core-level calculations at an acceptable computational cost, but also allows using diffusion theory for the flux solution.

Diffusion theory revisited: approximations and validity

As discussed in Lecture 4, diffusion theory is based on a number of approximations, in particular Fick's law, which couples together flux gradient and neutron current density:

$$\mathbf{J}_g(\boldsymbol{r},t) = -D_g \nabla \phi_g(\boldsymbol{r},t) \tag{1}$$

This allows writing the transport problem in the form of a balance equation using a single density-like function, Φ:[1]

$$\begin{aligned}\frac{1}{v_g}\frac{\partial}{\partial t}\Phi_g(\boldsymbol{r},t) - D_g\nabla^2\Phi_g(\boldsymbol{r},t) + \Sigma_{\mathrm{r},g}\Phi_g(\boldsymbol{r},t) = Q_g(\boldsymbol{r},t) + \sum_{g'\neq g}\Sigma_{\mathrm{s},g'g}\Phi_{g'}(\boldsymbol{r},t) \\ + \chi_g\sum_{g'}\nu\Sigma_{\mathrm{f},g'}\Phi_{g'}(\boldsymbol{r},t)\end{aligned} \tag{2}$$

The main approximations in the derivation of (2) can be summarized as:

1) Neutron flux can be linearized with respect to angular coordinates (linear anisotropy)
2) The medium is infinite and homogeneous
3) Scattering is the dominant reaction mode, and isotropic in the L-frame
4) Wide energy groups in multi-group condensation

[1] Solution to the neutron diffusion equation is denoted here with a capital phi, Φ. For clarity, Φ is referred to as the diffusion flux in contexts where it is easily confused with the scalar flux, ϕ, obtained from the solution of the transport equation.

Diffusion theory revisited: approximations and validity

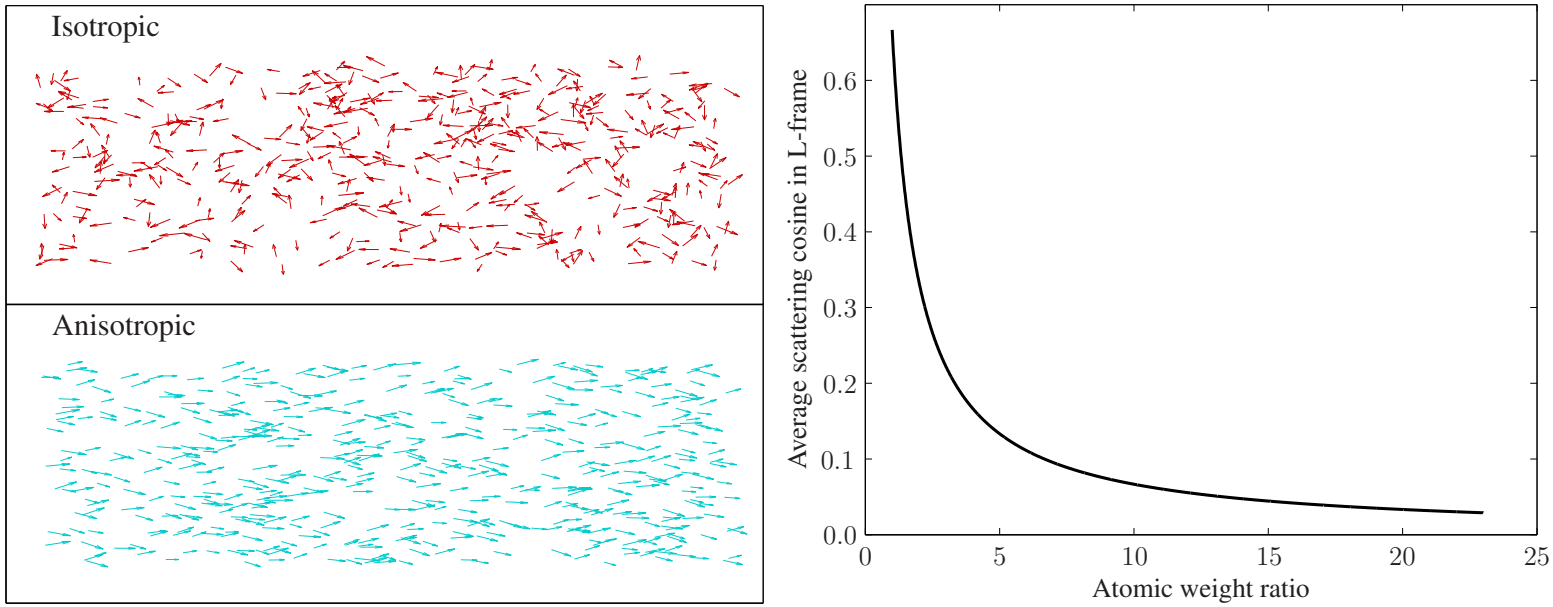

Figure 1 : Left: Illustration of an isotropic and anisotropic vector field, for example, neutron current density. In the isotropic case neutron directions are completely randomly distributed. In the anisotropic case there is a clear preferential direction. Right: Anisotropy of elastic potential scattering in the laboratory frame-of-reference (L-frame). Even though potential scattering is isotropic in the center-of-mass frame (C-frame), i.e. the average scattering cosine is zero, the anisotropy increases in the L-frame with decreasing nuclide mass. The curve shows that scattering from hydrogen, for example, has a clear forward bias.

Diffusion theory revisited: approximations and validity

Linear flux anisotropy is a poor approximation in or near:

1) Localized sources
2) Strong absorbers
3) Vacuum boundaries and low-density material regions
4) Large moderator regions

For strong absorbers and vacuum boundaries the anisotropy is caused by the lack of back-flow through the boundary surface. For large moderator regions there is a large inward component of fast neutrons and an outward component of thermal neutrons, which disrupts the flux isotropy.

Spatial homogenization at the fuel assembly level removes most of the problems caused by local heterogeneities:

- The geometry consists of homogeneous regions that are large compared to neutron mfp (good approximation to infinite homogeneous medium)
- Effects of localized strong absorbers in flux anisotropy are smoothed out
- Scattering becomes the dominant reaction mode when reaction probabilities are averaged over the local geometry

Diffusion theory revisited: approximations and validity

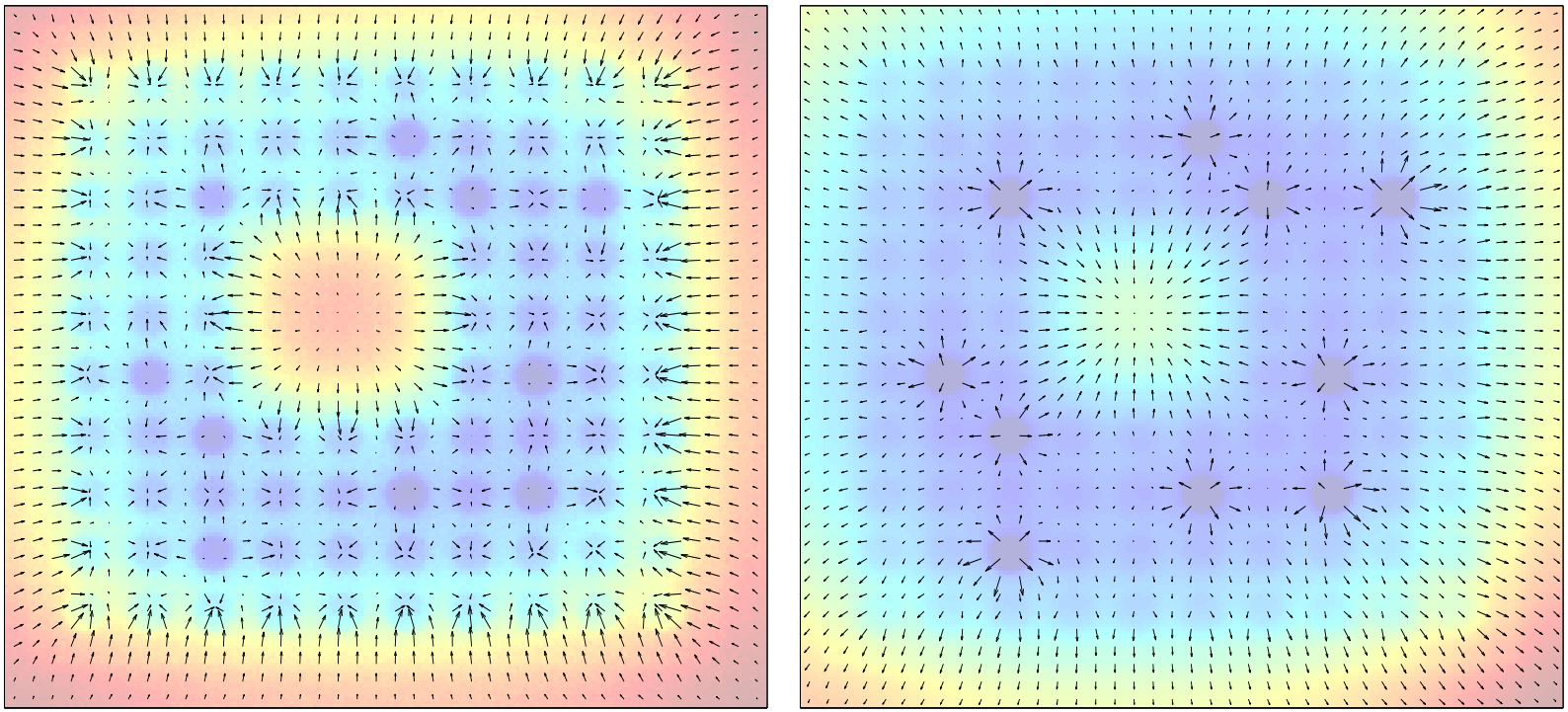

Figure 2 : Flux gradient field in fast (left) and thermal (right) energy group in a BWR fuel assembly, demonstrating the heterogeneity of the flux solution. Neutron density distribution is plotted in the background. Energy group boundary is set to 0.625 eV. Calculations carried out using Monte Carlo simulation.

Diffusion theory revisited: approximations and validity

Spatial homogenization does not change the fact that scattering is an anisotropic reaction in the L-frame,[2] in particular for light elements (See Fig. 5). Since more than 90% of all neutron interactions in LWR's consist of elastic scattering from hydrogen in water, the requirement of isotropic scattering is clearly not met.

This error is compensated to some extent by the transport-correction, which is seen in the definition of the transport cross section (out-scattering approximation):

$$\Sigma_{\mathrm{tr},h} \approx \Sigma_h - \overline{\mu}\,\Sigma_{\mathrm{s},h} \ , \tag{3}$$

used in the calculation of the diffusion coefficient:

$$D_g = \frac{\displaystyle\sum_{h\in g}\sum_i \frac{\Phi_{i,h}}{3\Sigma_{\mathrm{tr},i,h}}}{\displaystyle\sum_{h\in g}\sum_i V_i\Phi_{i,h}} \ . \tag{4}$$

In Lecture 4 the diffusion coefficient was associated with the distance migrated by the neutrons in a homogeneous medium, which is increased by scattering anisotropy ($\overline{\mu} > 0$). In a way, the directional component of the double-differential scattering rate is contained within the transport cross section, while the group-transfer cross section contains the energy-transfer component.

[2] Scattering isotropy in the L-frame must not be confused with isotropy in the C-frame, which is generally a good approximation.

Diffusion theory revisited: two-group diffusion calculations

LWR core simulations are most typically based on two-group diffusion theory, in which the thermal group covers the Maxwellian distribution of fully thermalized neutrons and the rest of the spectrum is contained within the fast group. The group boundary is typically set to 0.625 eV.

The two-group diffusion equations can be written by setting χ_1 = 1 and χ_2 = 0 and re-grouping some of the terms in (2). In the k-eigenvalue form the equations are written as:

$$\begin{aligned} -D_1\nabla^2\Phi_1(\boldsymbol{r}) + (\Sigma_{\mathrm{a},1} + \Sigma_{\mathrm{rem}})\,\Phi_1(\boldsymbol{r}) &= \frac{1}{k}\left[\nu\Sigma_{\mathrm{f},1}\Phi_1(\boldsymbol{r}) + \nu\Sigma_{\mathrm{f},2}\Phi_2(\boldsymbol{r})\right] \\ -D_2\nabla^2\Phi_2(\boldsymbol{r}) + \Sigma_{\mathrm{a},2}\Phi_2(\boldsymbol{r}) &= \Sigma_{\mathrm{rem}}\Phi_1(\boldsymbol{r}) \end{aligned} \tag{5}$$

where the contribution from up-scattering is included in the removal cross section:

$$\Sigma_{\mathrm{rem}} = \Sigma_{\mathrm{s},12} - \frac{\Phi_2}{\Phi_1}\Sigma_{\mathrm{s},21} \tag{6}$$

The time-dependent form of Eq. (5) also includes the external source and time-derivative terms, and the $1/k$ multiplier in the fission source is omitted. Delayed neutron emission couples the two-group diffusion equations into the delayed neutron precursor equations with additional fission source terms (see Lecture 2).

Diffusion theory revisited: two-group diffusion calculations

In two-group diffusion theory, all the complicated interaction physics within the homogenized region is contained in 7 group constants:

- Fast and thermal absorption cross section $\Sigma_{\mathrm{a},1}, \Sigma_{\mathrm{a},2}$, defining the total rate at which neutrons are removed from the population[3]
- Fast and thermal fission neutron production cross section $\nu\Sigma_{\mathrm{f},1}, \nu\Sigma_{\mathrm{f},2}$, defining the rate at which new neutrons are produced
- Fast and thermal diffusion coefficient D_1, D_2, characterizing the migration of neutrons in the homogeneous medium (and containing the angular-dependent part of the double-differential scattering rate)
- Removal cross section Σ_{rem}, describing the net down-scattering of neutrons from fast to thermal group (and containing the energy-dependent part of double-differential scattering rate)

Time-dependent diffusion calculations also include the inverse neutron speeds $1/v_1, 1/v_2$ and effective delayed neutron parameters. The time constants are weighted with adjoint neutron flux, as briefly noted in Lecture 2.

[3] Absorption in this context refers to all reactions in which the incident neutron is lost, including fission.

Diffusion theory revisited: spatial homogenization

The homogenization of reaction cross sections can be formally written as:

$$\Sigma_g = \frac{\int_V \int_{E_g}^{E_{g-1}} \Sigma(E)\phi(\boldsymbol{r}, E) dV dE}{\int_V \int_{E_g}^{E_{g-1}} \phi(\boldsymbol{r}, E) dV dE} \tag{7}$$

Where the integrals are carried over the energy group and the homogenized geometry. These integrals can be evaluated directly using Monte Carlo simulation, but the common approach is to use deterministic lattice transport codes, in which case the flux solution is obtained in multi-group space-discretized form. The homogenization procedure is then written as:

$$\Sigma_g = \frac{\sum_{h \in g} \sum_i V_i \Sigma_{i,h} \phi_{i,h}}{\sum_{h \in g} \sum_i V_i \phi_{i,h}} \tag{8}$$

where h refers to the multi-group division used in the heterogeneous solution and g to the final few-group division. Index i refers to spatial sub-division, such as the flat-source regions in MOC.

Alternatively, the geometry is first homogenized while maintaining the original multi-group structure (or some subset of it), after which a leakage-corrected spectrum is obtained by solving the B_1 equations. This spectrum is then used for collapsing the data into the final few-group form (see brief description of leakage corrections in Lecture 7).

Diffusion theory revisited: spatial homogenization

The diffusion coefficient is calculated by collapsing the inverse of the transport cross section:

$$D_g = \frac{\sum_{h\in g}\sum_i \frac{\phi_{i,h}}{3\Sigma_{\mathrm{tr},i,h}}}{\sum_{h\in g}\sum_i V_i\phi_{i,h}} \approx \frac{\sum_{h\in g}\sum_i \frac{\phi_{i,h}}{3(\Sigma_{i,h}-\overline{\mu}\,\Sigma_{\mathrm{s},i,h})}}{\sum_{h\in g}\sum_i V_i\phi_{i,h}} \tag{9}$$

where $\overline{\mu}$ is the average scattering angle in group h. The diffusion coefficient can also be obtained from the critical buckling with the solution of the B_1 equations.[4]

All information on isotopic compositions is lost in the process of homogenization, which means that burnup calculation has to be performed before proceeding to the next stage in the calculation chain.

Burnup calculation requires one-group transmutation cross sections used for forming the Bateman depletion equations, which can be calculated similar to (8):

$$\sigma = \frac{\sum_h \sigma_h\phi_h}{\sum_h \phi_h} \tag{10}$$

[4] For details, see: R. Stamm'ler and M. Abbate, "Methods of Steady-State Reactor Physics in Nuclear Design." Academic Press Inc. 1983.

Diffusion theory revisited: spatial homogenization

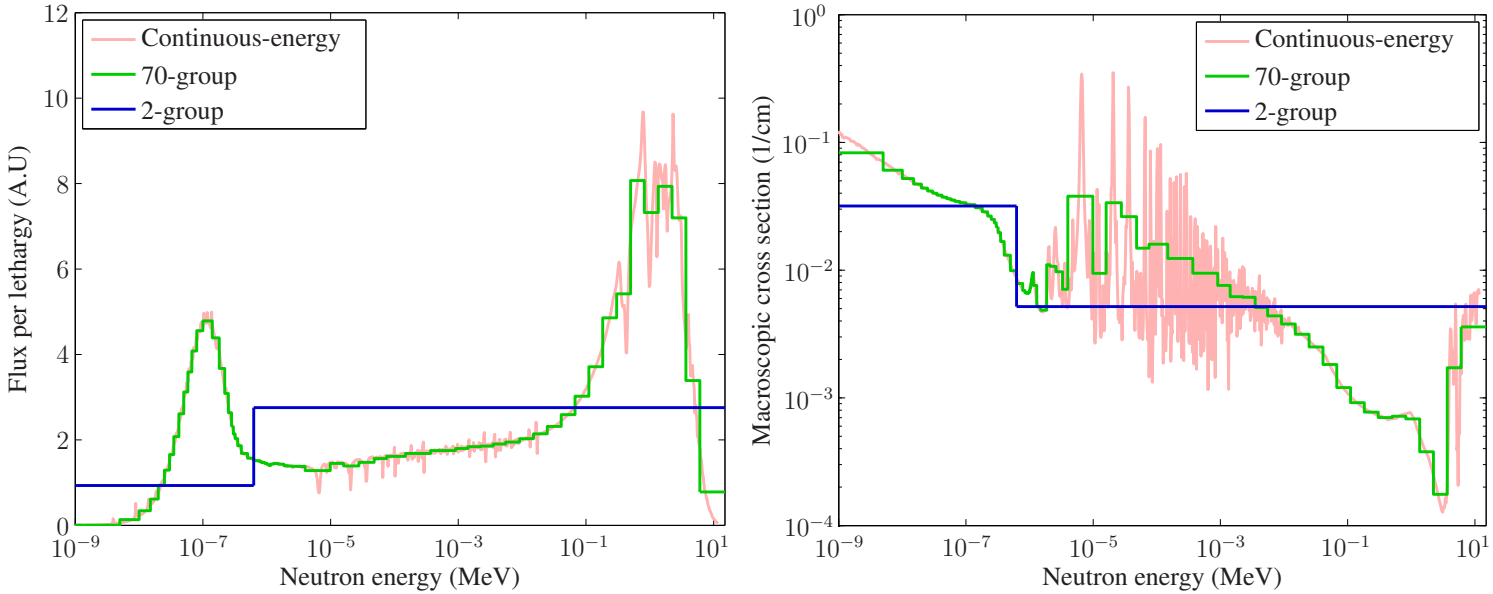

Figure 3 : Illustration of energy group condensation for flux (left) and total absorption cross section (right). Condensation of flux is performed by integration over energy groups. Condensation of cross sections is carried out by calculating flux-volume-weighted averages that preserve the reaction rate balance as in Eq. (8).

Full-core calculations

The core geometry is divided into homogeneous calculation nodes, typically the size of a single fuel assembly divided into 20-30 axial zones.[5] The cross sections for each node are obtained from spatial homogenization, which provides the "building blocks" for the full-scale model.

The core-level calculation is based on the following assumptions:

- The reactor physical characteristics depend mainly on the assembly type and the local operating conditions (fuel burnup, thermal-hydraulic state)
- The position of the assembly affects neutronics only indirectly, via the coupling between local power and thermal hydraulics
- The heterogeneity of the core is limited to radial dimensions, the reactor physical characteristics of fuel do not change sharply in the axial direction

The last assumption is a simplification resulting from the traditional design of fuel assemblies. There are also axially heterogeneous cores where this assumption does not hold.

It should be noted that full-core calculation is a diverse topic, covering a multitude of implementations and solution methods. What is presented in the following is a generalization, demonstrating the basic concepts of nodal methods, equivalence theory and the use of discontinuity factors.

[5] If the node size is too small, the validity of diffusion theory may be compromised. If the size is too large, the solution fails to represent the spatial variation in flux and reaction rate.

Full-core calculations

The terminology related to full-core calculations can be somewhat confusing. The methodology deals with two types of transport problems:

1) Heterogeneous problem – detailed description of geometry at assembly or core level
2) Homogeneous problem – homogenized description of geometry at assembly or core level

and two spatial scales:

1) Local scale – single fuel assembly (separated from its surroundings)
2) Global scale – core level

This results in four types of flux solutions:

1) Local heterogeneous flux, ϕ
2) Local homogeneous (diffusion) flux, Φ
3) Global homogeneous (diffusion) flux, $\hat{\Phi}$
4) Global heterogeneous flux, $\hat{\phi}$

The heterogeneous flux solution requires higher-order transport methods, and the homogeneous problem is solved using simplified techniques, such as diffusion theory. All solutions are assumed to exist, even though the last one cannot be obtained in practice.

Full-core calculations

Local heterogeneous flux, ϕ

- Solution to the local heterogeneous transport problem
- Obtained by deterministic transport codes using a detailed 2D description of a single fuel assembly
- 40, 70, 172, 238 (or so) energy groups
- Used for producing homogenized few-group constants

Global heterogeneous flux, $\hat{\phi}$

- Solution to the global heterogeneous transport problem
- The actual solution to the full-scale problem that exists but is never reached

Local homogeneous (diffusion) flux, Φ

- Solution to the local homogeneous transport problem
- Obtained by solving the few-group diffusion equation in homogenized assembly-level geometry

Global homogeneous (diffusion) flux, $\hat{\Phi}$

- Piece-wise continuous solution to the global homogeneous transport problem
- Obtained by coupling intra-nodal homogeneous diffusion flux solutions together by continuity conditions
- Represents the solution to the full-scale transport problem

Full-core calculations

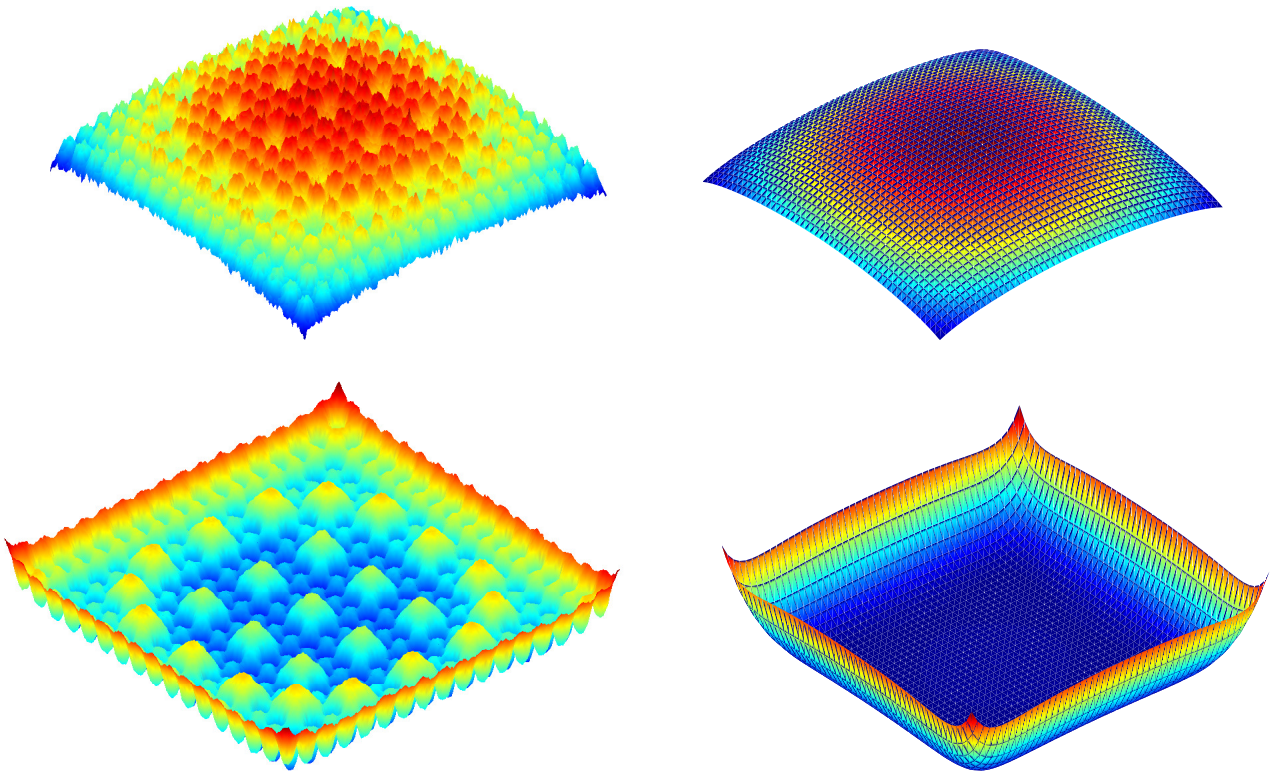

Figure 4 : Illustration of heterogeneous and homogeneous flux inside a single fuel assembly. Top left: fast heterogeneous flux, Top right: fast homogeneous flux, Bottom left: thermal heterogeneous flux, bottom right: thermal homogeneous flux.

Discontinuity factors and equivalence theory

Even though the global heterogeneous and homogeneous flux are solutions to different problems, they represent the same reaction rate distribution at the nodal level.[6] The two solutions are also assumed to be coupled to each other at the node boundaries via so-called assembly discontinuity factors (ADF's):

$$f_{g,k} = \frac{\hat{\phi}_{g,k}}{\hat{\Phi}_{g,k}} \tag{11}$$

where g is the energy group and k refers to a segment of the node boundary (most commonly a node face) where the coupling is applied and over which the two fluxes are averaged.

If the two nodes on the two sides of surface k are denoted with $-$ and $+$, the continuity of heterogeneous flux can be written as:

$$\hat{\phi}^{-}_{g,k} = \hat{\phi}^{+}_{g,k} \tag{12}$$

from which it results that the homogeneous flux is coupled by:

$$f^{-}_{g,k}\hat{\Phi}^{-}_{g,k} = f^{+}_{g,k}\hat{\Phi}^{+}_{g,k} \tag{13}$$

where $f^{-}_{g,k}$ and $f^{+}_{g,k}$ are the ADF's calculated for the nodes on the two sides of surface k.[7]

[6] This is how spatial homogenization was performed.

[7] It is important to note here that $f^{-}_{g,k}$ and $f^{+}_{g,k}$ are two different numbers, because the homogeneous flux is not continuous over the boundary (hence the name discontinuity factor).

Discontinuity factors and equivalence theory

The global homogeneous flux, $\hat{\Phi}$, is what the whole procedure is aiming to solve and the fact that the global heterogeneous flux, $\hat{\phi}$, cannot be solved was the reason to turn to simplified methods in the first place. So how to obtain the discontinuity factors?

The solution is to assume *equivalence* between the local and global flux, i.e. that the results of the assembly-level calculation represent the results of the full-core calculation inside the same assembly type in same conditions.

The assembly discontinuity factor (11) can then be defined using the local flux variables as:

$$f_{g,k} \approx \frac{\phi_{g,k}}{\Phi_{g,k}} \tag{14}$$

The local heterogeneous flux, $\phi_{g,k}$, is obtained from the same assembly calculation that produced the group constants, by collapsing the micro-group structure into the few-group structure and integrating over segment k. The local homogeneous flux $\Phi_{g,k}$ is discussed shortly.

It should be noted that the same equivalence was actually already applied in the production of homogenized group constants, since the cross sections were weighted with ϕ, not $\hat{\phi}$, and it results from the previous assumptions that the reactor physical characteristics are more dependent on the assembly type and local operating conditions and less on the position of the assembly within the core.

Discontinuity factors and equivalence theory

It is important to note that even though the local homogeneous flux, Φ, was defined earlier, it has so far only been used in the definition of the assembly discontinuity factor in Eq. (14). In particular, it is not the same thing as the intra-nodal homogeneous flux solution, which makes up the global homogeneous flux, $\hat{\Phi}$.

The local homogeneous flux is instead the local equivalent of the intra-nodal homogeneous flux, i.e. the solution to the diffusion equation in the *homogenized* assembly-level geometry.

Since both are solutions to the diffusion problem in homogeneous medium, characterized by the same group constants, the only thing that separates the two are the boundary conditions:

- In the global homogeneous problem the boundary conditions are the continuity conditions used to couple adjacent intra-nodal solutions together
- In the local homogeneous problem the boundary conditions depend on how the assembly-level geometry is set up

So similar to homogenized group constants, the discontinuity factors can also be obtained from the assembly-level calculation, but the exact procedure depends on the boundary conditions.

Discontinuity factors and equivalence theory

The definition of the ADF in Eq (14) is written with the flux integrals as:

$$f_{g,k} = \frac{\phi_{g,k}}{\Phi_{g,k}} = \frac{\frac{1}{S_k}\int_{S_k}\int_{E_g}^{E_{g-1}} \phi(\boldsymbol{r}, E) dS dE}{\frac{1}{S_k}\int_{S_k} \Phi_g(\mathbf{r}) dS} \tag{15}$$

where S_k is the area of surface k.

As mentioned earlier, spatial homogenization is most commonly performed using reflective boundary conditions, which corresponds to an infinite array of identical fuel assemblies.

Each neutron crossing the outer boundary is reflected back, which means that inward and outward currents cancel each other, resulting in zero net current over the assembly boundaries.

According to Fick's law (1), this means that also the flux gradient is zero at the boundary:

$$\mathbf{J}_g = 0 \Longrightarrow \nabla \phi_g = 0 \tag{16}$$

Since the geometry consists of homogeneous medium, there is nothing to change the flux shape, which implies that:

> *When spatial homogenization is performed using reflective boundary conditions, the homogeneous flux solution is constant over the entire volume.*

Discontinuity factors and equivalence theory

Since the flux is constant, the average over any boundary surface must be equal to the average over the entire volume:

$$\frac{1}{S_k}\int_{S_k}\Phi_g(\mathbf{r})dS = \frac{1}{V}\int_V \Phi_g(\mathbf{r})dV \tag{17}$$

The preservation of reaction rates in turn necessitates that the volume-averaged homogeneous flux is equal to the volume-averaged heterogeneous flux:

$$\frac{1}{V}\int_V \Phi_g(\mathbf{r})dV = \frac{1}{V}\int_V \int_{E_g}^{E_{g-1}} \phi(\boldsymbol{r},E)dVdE \tag{18}$$

Combining the results of Eqs. (15), (17) and (18) gives:

$$f_{g,k} = \frac{\frac{1}{S_k}\int_{S_k}\int_{E_g}^{E_{g-1}} \phi(\boldsymbol{r},E)dSdE}{\frac{1}{V}\int_V \int_{E_g}^{E_{g-1}} \phi(\boldsymbol{r},E)dVdE} \tag{19}$$

In other words, if the fuel assembly is homogenized with reflective boundary conditions, the ADF's can be calculated as the ratio of surface-averaged to volume-averaged heterogeneous flux. The local homogeneous flux is then not needed at all.

Discontinuity factors and equivalence theory

Infinite-lattice calculations with reflective boundary conditions are a good approximation if the heterogeneous flux gradient between adjacent assemblies is known to be small. This may not be the case for:

1) Assemblies located at the core-reflector boundary
2) Assemblies located adjacent to very reactive or absorbent assemblies (for example, mixed UOX/MOX loading)

In such case, the homogenized assembly can be modeled with its immediate surroundings, for example, in a “colorset” configuration (see Fig. 9).

This removes the reflective boundary and ADF’s must be calculated from (15), with an explicit solution to homogeneous flux, obtained by using net currents (provided by the heterogeneous flux solution) as the boundary conditions.[8]

Non-zero net-current boundary conditions are also encountered in reflector and some control absorber geometries, for which the only net source of neutrons is the inward current from the surrounding fuel.

[8] It is important that the local homogeneous flux is solved using the same methods and approximations as used for solving the global homogeneous problem in the nodal diffusion code.

Nodal diffusion methods

Because the geometry is homogeneous inside each node, the shape of the intra-nodal diffusion flux solution depends only on boundary conditions at the node boundary.

The general idea in nodal diffusion calculation is to describe the intra-nodal homogeneous diffusion flux using group-wise shape functions, and apply a number of continuity conditions that couple the node-wise solutions to each other, forming the global homogeneous flux.

The boundary conditions for the intra-nodal flux solution are determined by:

1. Continuity of current over node boundaries
2. Continuity of global heterogeneous flux over node boundaries
3. Coupling between global heterogeneous flux to global homogeneous flux at node boundaries (via discontinuity factors)

It is important to note that the continuity of flux applies only to the global heterogeneous solution, which is assumed to exist, but cannot be obtained computationally. The continuity of the global homogeneous flux is relaxed, and the boundary values are instead coupled to the heterogeneous flux using discontinuity factors.

The number and type of boundary conditions and the way in which this solution is written depends on the implementation.

Nodal diffusion methods

Nodal diffusion methods have been developed over a period of several decades, and limited computer capacity has affected the practical implementation in calculation codes. The topic covers a wide range of models, approximations and algorithms.[9]

The most significant differences between different nodal methods can be attributed to:

Treatment of the axial dimension:

- Separation of radial and axial solutions
- Transverse integration
- True 3D solution (AFEN / FENM)

Representation of shape functions:

- Polynomial approximation
- Exact solution to diffusion equations

Other determining factors include number of energy groups and applicability of the solution to different geometry types (square vs. hex).

The following example represents an AFEN-type (Analytical Function Exansion Nodal) solution.

[9] For a general description, see: W. M. Stacey, *"Nuclear Reactor Physics,"* Wiley, 2001.

Nodal diffusion methods

The multi-group diffusion equation can be written in matrix form as:

$$-\mathbf{D}\nabla^2\hat{\mathbf{\Phi}} + \mathbf{\Sigma}\hat{\mathbf{\Phi}} = \mathbf{\Sigma}_\mathrm{s}\hat{\mathbf{\Phi}} + \frac{1}{k}\chi(\nu\mathbf{\Sigma}_\mathrm{f})^T\hat{\mathbf{\Phi}} \tag{20}$$

where the coefficients are constant matrices and $\hat{\mathbf{\Phi}}$ is a vector containing the flux in each group. This equation is simplified into the Helmholtz equation in matrix form:

$$\nabla^2\hat{\mathbf{\Phi}} = \mathbf{M}\hat{\mathbf{\Phi}} \tag{21}$$

where:

$$\mathbf{M} = \mathbf{D}^{-1}\mathbf{A} \tag{22}$$

and

$$\mathbf{A} = \mathbf{\Sigma} - \mathbf{\Sigma}_\mathrm{s} - \frac{1}{k}\chi(\nu\mathbf{\Sigma}_\mathrm{f})^T \tag{23}$$

The solution in Cartesian coordinates can be written as:

$$\mathbf{f}(x,y,z) = e^{\mathbf{B}_1 x + \mathbf{B}_2 y + \mathbf{B}_3 z}\mathbf{c} \tag{24}$$

where $\mathbf{c}$ is a constant vector and:

$$\mathbf{B}_1^2 + \mathbf{B}_2^2 + \mathbf{B}_3^2 = \mathbf{M} \tag{25}$$

Functions of the form (24) are called the basis functions of the flux solution.

Nodal diffusion methods

In theory, there is an infinite number of basis functions that satisfy Eq. (20) with condition (25), for example:

$$\begin{aligned} B_2 = 0; B_3 = 0 &\Rightarrow \mathbf{f}(x) = e^{\pm\sqrt{\mathbf{M}}x}\mathbf{c} \\ B_3 = 0; B_1 = B_2 &\Rightarrow \mathbf{f}(x,y) = e^{\pm\sqrt{\frac{\mathbf{M}}{2}}(x+y)}\mathbf{c} \end{aligned} \tag{26}$$

The general solution is a linear combination of all basis functions. In practice, the number of terms is limited by the number of continuity conditions, and the selection is based on the problem and geometry type (for example, square vs. hexagonal fuel lattice).

In two dimensional square lattice the solution could be written as:

$$\hat{\Phi}(x,y) = e^{\sqrt{\mathbf{M}}x}\mathbf{c}_1 + e^{-\sqrt{\mathbf{M}}x}\mathbf{c}_2 + e^{\sqrt{\mathbf{M}}y}\mathbf{c}_3 + e^{-\sqrt{\mathbf{M}}y}\mathbf{c}_4 \tag{27}$$

and coefficient vectors $\mathbf{c}_1, \mathbf{c}_2, \mathbf{c}_3, \mathbf{c}_4$ would be fixed by the continuity conditions applied at each node face.

By providing additional continuity conditions for currents at node corners the solution could be written as:

$$\begin{aligned} \hat{\Phi}(x,y) =& e^{\sqrt{\mathbf{M}}x}\mathbf{c}_1 + e^{-\sqrt{\mathbf{M}}x}\mathbf{c}_2 + e^{\sqrt{\mathbf{M}}y}\mathbf{c}_3 + e^{-\sqrt{\mathbf{M}}y}\mathbf{c}_4 \\ &+ e^{\sqrt{\mathbf{M}}(x+y)}\mathbf{c}_5 + e^{-\sqrt{\mathbf{M}}(x+y)}\mathbf{c}_6 + e^{\sqrt{\mathbf{M}}(x-y)}\mathbf{c}_7 + e^{-\sqrt{\mathbf{M}}(x-y)}\mathbf{c}_8 \end{aligned} \tag{28}$$

The choice of basis functions is basically arbitrary, but it does effect the accuracy of the solution. By including additional continuity conditions for corner currents allows more accurate description of diagonal spatial dependence.

Nodal diffusion methods

The continuity of current in group g over boundary k is written as:

$$\int_{S_k} \mathbf{J}_g^-(\boldsymbol{r}) \cdot d\mathbf{S} = \int_{S_k} \mathbf{J}_g^+(\boldsymbol{r}) \cdot d\mathbf{S} \tag{29}$$

or applying Fick's law:

$$\int_{S_k} D_g^- \nabla \hat{\Phi}_g^-(\boldsymbol{r}) \cdot d\mathbf{S} = \int_{S_k} D_g^+ \nabla \hat{\Phi}_g^+(\boldsymbol{r}) \cdot d\mathbf{S} \tag{30}$$

The continuity of heterogeneous flux is written as

$$\int_{S_k} \hat{\phi}_g^-(\boldsymbol{r}) dS = \int_{S_k} \hat{\phi}_g^+(\boldsymbol{r}) dS \tag{31}$$

from which the discontinuity of the homogeneous flux can be written using the discontinuity factors:

$$\int_{S_k} f_g^- \hat{\Phi}_g^-(\boldsymbol{r}) dS = \int_{S_k} f_g^+ \hat{\Phi}_g^+(\boldsymbol{r}) dS \tag{32}$$

Nodal diffusion methods

The continuity of current and discontinuity of homogeneous flux provide the sufficient equations for fixing the unknown amplitude coefficients of the basis functions.

This is best seen by considering a system consisting of two rectangular nodes, for which the two-group intra-nodal flux solutions are written using 4 basis functions per group as in as (27):

- The total number of unknown coefficients is 16 (2 nodes, 2 energy groups 4 basis functions per group)
- The outer boundary conditions fix 12 unknown coefficients (6 outer faces, 2 energy groups)
- The continuity of current at node boundary fixes 2 coefficients (1 equation per group)
- The discontinuity of flux at node boundary fixes 2 coefficients (1 equation per group)

The outer boundary conditions are typically vacuum, which is a good approximation if the active core is surrounded by sufficient amount of non-multiplying reflector.

Discontinuity factors are traditionally not used at axial node boundaries, which essentially assumes continuity of homogeneous flux. This is a good approximation if the material properties do not exhibit sharp discontinuities. This assumption may lead to errors near control rod tips[10] and in assemblies with axially-profiled burnable absorber pins.

[10] The movement of control rods is not limited to node boundaries. Partial insertion within a node is accounted for by axial re-homogenization, which averages the reactivity effect over the entire node volume.

Pin-power reconstruction

Since the global homogeneous flux $\hat{\Phi}$ literally represents the solution to a homogenized problem, it can provide information on the core power distribution only at node level. Since various safety margins are based on the maximum temperature of the hottest pin, it is necessary to calculate the power distribution also at pin level.

This can be accomplished by pin-power reconstruction, which means combining the homogeneous intra-nodal flux to form factors that represent the power distribution inside the assembly. These form factors are obtained from the assembly-level calculation together with other group constants:

$$p_{g,j} = \frac{\sum_{h \in g} \kappa \Sigma_{\mathrm{f},h,j} \phi_{h,j}}{\Phi_{g,j}} \tag{33}$$

where $\kappa\Sigma_{\mathrm{f}}$ is the fission energy production cross section and j is the pin index.

The local pin-powers are then obtained by multiplying the form factors with the global homogeneous flux from the full-core calculation and summing over energy groups:

$$P_j = \sum_g p_{g,j} \hat{\Phi}_{g,j} \tag{34}$$

The local homogeneous flux Φ is obtained as in the calculation of ADF's – if the assembly is surrounded by reflective boundary conditions, the flux is constant, if not it requires solution to the homogenized problem with non-zero net current boundary conditions.

Parametrization of group constants

As mentioned above, the dependence of interaction probabilities on fuel burnup and local thermal hydraulic state is lost in the process of homogenization, as the heterogeneous geometry and isotopic micro-group cross sections are replaced by macroscopic homogeneous group constants.

This information is recovered by repeating the procedure in such way that all reactor operating conditions are covered. The result is a parametrized library of group constants, from which the values corresponding to the local state can be obtained by interpolation.

Since the local operating conditions inside a fuel assembly also affect how the assembly is depleted, the state-points by which the group constant data is parametrized are not completely independent. The calculations are instead divided into:

Branch variations – taking into account the momentary changes in the operating conditions: fuel temperature, moderator density and temperature, boron concentration, insertion of control rods

History variations – taking into account conditions that persist for an extended period of time, affecting the way the fuel is burnt: moderator temperature and density, boron concentration, position of control rods

History variations are handled by running separate burnup calculations, and branch variations by performing restarts to the given states.

Parametrization of group constants

Examples of branch variations:

- Fuel temperature varied between cold core (300 K), nominal operating temperature (850 K) and elevated state (1500 K)
- Coolant temperature and density varied between cold core (300 K), average (560 K) and high (600 K)
- Boron concentration varied between zero, cycle average (500 ppm) and high (2000 ppm)
- Control rods inserted and withdrawn

One state corresponds to nominal operating condition and the remaining two to extreme conditions on both sides.

Examples of history variations:

- Coolant temperature and density varied between core inlet (550 K), core average (575 K) and core outlet (600 K)
- Boron concentration varied between beginning of cycle (1000 ppm), cycle average (500 ppm) and end of cycle (0 ppm)
- Presence of control rods in BWR's[11]

[11] PWR's are typically operated all rods out, which means that the presence of control rods has no impact on fuel depletion.

Parametrization of group constants

The dependence of cross sections on state variables can be taken into account by interpolating between tabulated values or using polynomial fits, for example:

$$\Sigma = \Sigma_0 + cT_\mathrm{f}^2 + dT_\mathrm{f} \tag{35}$$

where Σ_0 is the nominal state value, T_f is the variation in fuel temperature compared to nominal value[12] and c and d are two polynomial coefficients obtained by fitting a parabola on the data.

The variations can be considered independent of each other, or correlations can be accounted for using cross terms:

$$\Sigma = \Sigma_0 + eT_\mathrm{m}^2 + fT_\mathrm{m} + lB^2 + mB + pB^2T_\mathrm{m}^2 + qB^2T_\mathrm{m} + vBT_\mathrm{m}^2 + wBT_\mathrm{m} \tag{36}$$

where T_m is the variation in moderator temperature, B is the variation in boron concentration and e, f, l, m, p, q, v and w are coefficients obtained by fitting a second-order surface on the data.

Polynomial interpolation works well especially when the cross sections dependent (almost) linearly on the state variables. Problems can occur when the changes are sharp or interpolation turns to extrapolation, i.e. when the local state is beyond the extremes.

There are major differences between codes on how the parametrization is done in practice.

[12] Cross sections are also often parametrized as function of square root of fuel temperature.

Parametrization of group constants

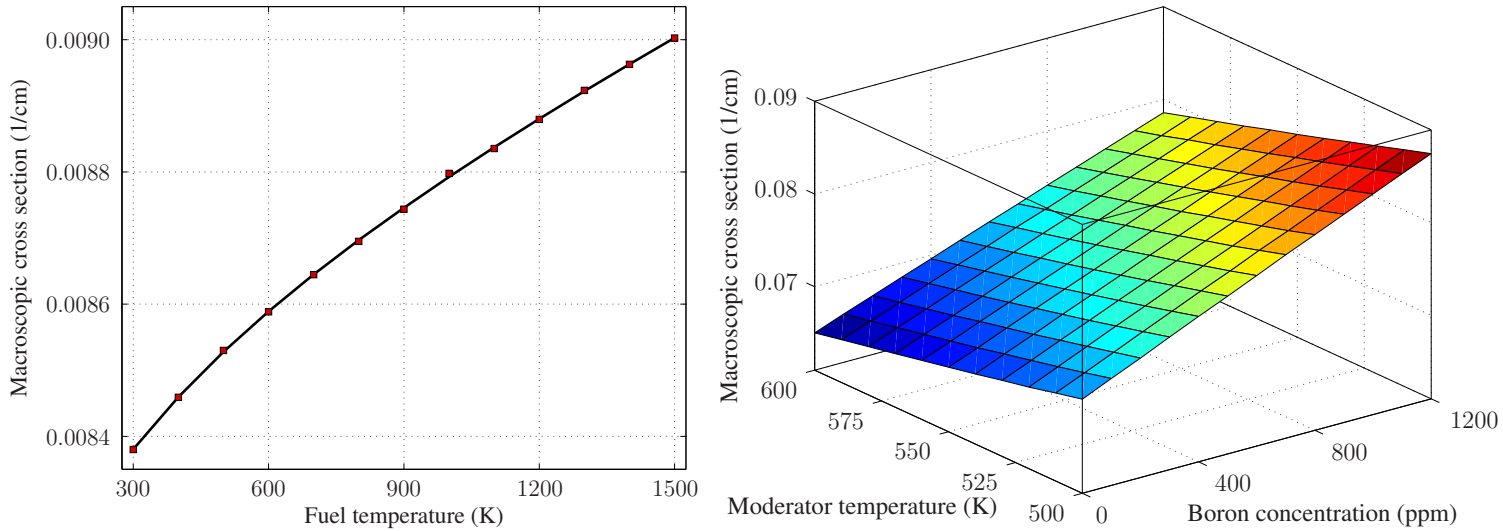

Figure 5 : Dependence of homogenized group constants on state variables in a PWR assembly calculation. Left: Fast-group absorption cross section ($\Sigma_{\mathrm{a},1}$) as function of fuel temperature. Second-order polynomial fit and discrete values from assembly calculation. Right: Dependence of thermal-group absorption cross section ($\Sigma_{\mathrm{a},2}$) on moderator temperature and boron concentration.

History variations

The main reason why cross sections depend on operating history is that the flux spectrum has a significant impact on plutonium build-up. In BWR's, for example, more plutonium is produced in the upper part of the assembly where void fraction is high and the spectrum is harder.

The effect is less pronounced in PWR's, in which the variation in coolant density is smaller. Coolant boron concentration also affects the spectrum and plutonium build-up.

Burnup calculations are run at the fuel assembly level from fresh fuel to discharge burnup. Maximum assembly-averaged burnup is typically 40-60 MWd/kgU, but the local maximum can be somewhat higher because of non-uniform axial flux shape.

The total number of transport solutions involved in group constant generation depends on the number of assembly types, history calculations, burnup points and combinations of branches. Covering all operating conditions typically requires thousands of runs.

A practical example is provided at the end of the lecture.

History variations

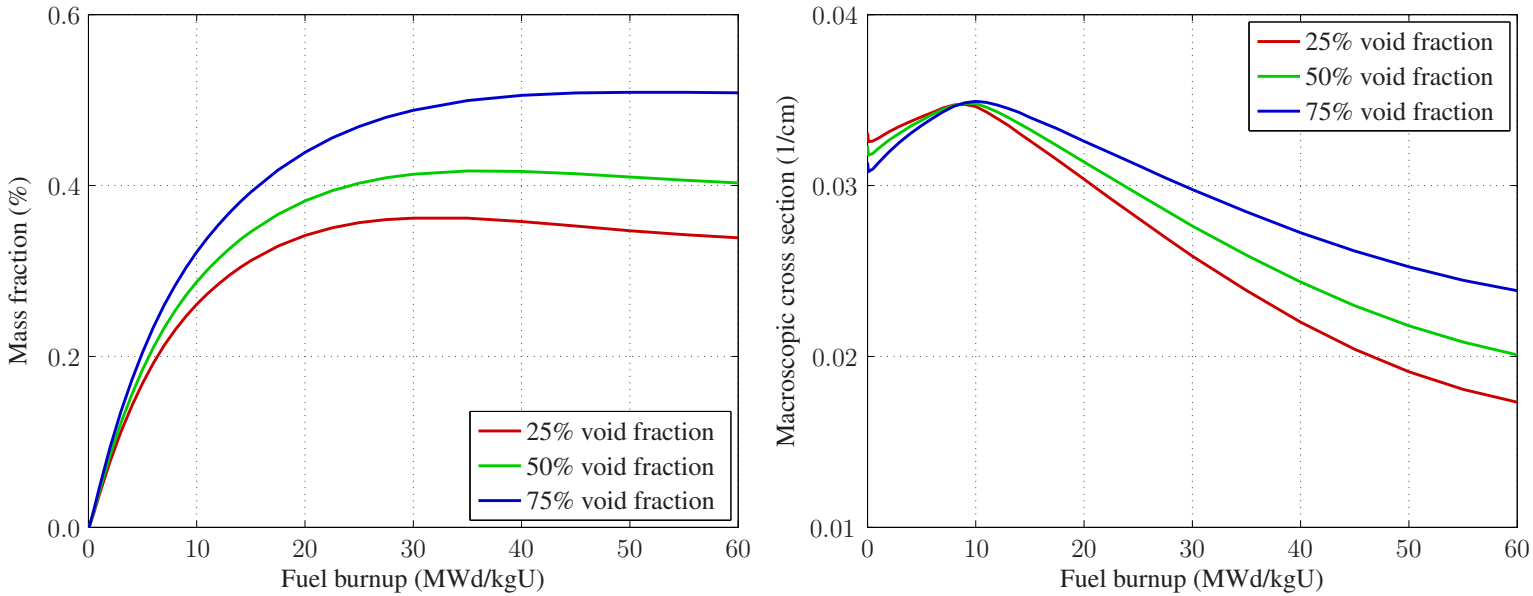

Figure 6 : Effect of coolant void fraction on plutonium build-up. Left: Mass fraction of ^{239}Pu as function of burnup in a BWR fuel assembly with burnable absorber and 25%, 50% and 75% void fraction. Harder spectrum leads to higher plutonium build-up. Right: Homogenized thermal fission cross section ($\Sigma_{\mathrm{f},2}$) as function of fuel burnup. Differences in plutonium build-up rate are taken into account in group constant generation by separate void history variations.

Fission product poisons

Since the concentrations of ^{135}Xe and ^{149}Sm depend on local fission power and immediate operating history, their contribution to total absorption cannot be fully accounted for in spatial homogenization. The solution is to track poison concentrations explicitly, which allows simulating fission product poisoning and xenon oscillations at core level.

This requires the calculation of additional homogenized few-group constants needed for forming the associated concentration equations:

- Fission yields of ^{135}I and ^{135}Xe: $\gamma_{\mathrm{I}}, \gamma_{\mathrm{X}}$. The yield of ^{135}I is cumulative, i.e. it includes the production of all short-lived precursors in the 135 mass chain.
- Microscopic capture cross sections of ^{135}Xe: $\sigma_{\mathrm{X},g}$. The capture in ^{135}I is usually omitted.
- Macroscopic fission cross sections: $\Sigma_{\mathrm{f},g}$, although this can also be combined with the isotope yields.[13]

In addition, the contribution of ^{135}Xe in macroscopic total absorption in the homogenized assembly is represented by a separate xenon absorption cross section Σ_{X}.

Similar parameters can be provided for ^{149}Sm and its precursor ^{149}Pm.

[13] The formulation of group diffusion equations involve fission neutron production cross section $\nu\Sigma_{\mathrm{f},g}$ and thermal hydraulics coupling requires fission energy production cross section $\kappa\Sigma_{\mathrm{f},g}$. The production terms for ^{135}I and ^{135}Xe can be similarly expressed with single constants: $\gamma_{\mathrm{I}}\Sigma_{\mathrm{f},g}$ and $\gamma_{\mathrm{X}}\Sigma_{\mathrm{f},g}$.

Fission product poisons

The Bateman equations for iodine (I) and xenon (X) concentration are written as:

$$\begin{aligned}\frac{dI}{dt} &= \gamma_{\mathrm{I}} \left(\Phi_1 \Sigma_{\mathrm{f},1} + \Phi_2 \Sigma_{\mathrm{f},2}\right) - \lambda_I I \\ \frac{dX}{dt} &= \gamma_{\mathrm{X}} \left(\Phi_1 \Sigma_{\mathrm{f},1} + \Phi_2 \Sigma_{\mathrm{f},2}\right) + \lambda_I I - \lambda_X X - \left(\Phi_1 \sigma_{\mathrm{X},1} + \Phi_2 \sigma_{\mathrm{X},2}\right) X\end{aligned} \tag{37}$$

where λ_{I} and λ_{X} are the decay constants of ^{135}I and ^{135}Xe, respectively.

The solution provides the node-wise concentration of ^{135}Xe, which can be used to calculate its contribution to total absorption:

$$\begin{aligned}\Sigma'_{\mathrm{a},1} &= \Sigma_{\mathrm{a},1} - \Sigma_{\mathrm{X},1} + \sigma_{\mathrm{X},1} X \\ \Sigma'_{\mathrm{a},2} &= \Sigma_{\mathrm{a},2} - \Sigma_{\mathrm{X},2} + \sigma_{\mathrm{X},2} X\end{aligned} \tag{38}$$

where Σ_{X} is the contribution of ^{135}Xe to macroscopic absorption cross section in the homogenized assembly.

The equilibrium concentration of ^{135}Xe is given by (see Lecture 5):

$$\lim_{t \to \infty} X(t) = \frac{\left(\Phi_1 \Sigma_{\mathrm{f},1} + \Phi_2 \Sigma_{\mathrm{f},2}\right)\left(\gamma_{\mathrm{I}} + \gamma_{\mathrm{X}}\right)}{\lambda_X + \Phi_1 \sigma_{\mathrm{X},1} + \Phi_2 \sigma_{\mathrm{X},2}} \tag{39}$$

which can be used to replace the instantaneous concentration when the reactor has been operating at constant power for several days.

Accuracy of full-core simulations

The accuracy of the full-core simulation depends on the validity of methods and approximations at various stages of the calculation chain, including:

- Accuracy of the fundamental interaction data in the evaluated nuclear data files
- Accuracy of spectral calculation and approximations, for example, taking into account the spatial and resonance self-shielding effects
- Accuracy of the heterogeneous transport solution used for spatial homogenization, and the related approximations (infinite lattices vs. colorset, etc.)
- Parametrization of group constants
- Solution of heat transfer and coolant flow
- Validity of diffusion theory in the full-scale calculation
- Accuracy of the nodal diffusion model or similar used for obtaining the full-scale flux solution

Despite the various crude approximations, it is possible to reach a very good level of accuracy for the neutronics solution (errors in nodal power $\sim$1%). The dominant error source in coupled calculations is often thermal hydraulics, especially in transients.

Example of spatial homogenization and core simulation

Example 1: MIT BEAVRS Benchmark with Serpent-ARES

The Serpent-ARES calculation sequence is applied in full-core simulations of a 1000 MWe Westinghouse PWR reactor:

- Spatial homogenization performed using the Serpent Monte Carlo code developed at VTT
- Full-core calculation carried out using the ARES nodal diffusion code developed at the Finnish Radiation and Nuclear Safety Authority (STUK)

The study is divided in three parts:

(i) Steady-state neutronics calculation for the hot zero-power (HZP) initial core, with comparison of power distributions to reference Serpent 3D calculation

(ii) Calculation of control rod worths and critical boron concentrations for the HZP state, and comparison of hot full-power (HFP) power distributions to Serpent 3D calculation

(iii) Simulation of first operating cycle and comparison of boron let-down curve to experimental data provided with the benchmark

This study was carried out within the SAFIR 2014 and SAFIR 2018 research programmes, with the purpose of validating the Serpent-ARES calculation sequence, and demonstrating that continuous-energy Monte Carlo simulation is a viable option for spatial homogenization.

Example of spatial homogenization and core simulation

Example 1: MIT BEAVRS Benchmark with Serpent-ARES

A few notes on the calculation tools...

Monte Carlo codes are not commonly used for spatial homogenization, but as long as the details are not too much concerned, this example can be considered a good demonstration of the calculation sequence and the related challenges.

The main advantages of using Monte Carlo codes for homogenization can be summarized as:

- No major approximations in geometry and physics, capable of handling complicated 3D geometries.
- The best available knowledge on neutron interactions can be used almost as-is, without spectral calculation and multi-group condensation with self-shielding effects
- The same code and cross section data can be used to provide a reference solution for validation, without additional uncertainties

The major challenges are related to the computational cost and the fact that covering all state points requires systematic management of a huge amount of data. Even though Serpent is specifically intended for spatial homogenization, the methodology is still under development.

ARES is a somewhat traditional state-of-the-art core simulator code, based on the analytical function expansion nodal (AFEN) method.

Example of spatial homogenization and core simulation

Example 1: MIT BEAVRS Benchmark with Serpent-ARES

The test case is the MIT BEAVRS benchmark:

`http://crpg.mit.edu/pub/beavrs`

The benchmark was initiated mainly for the purpose of validating high-fidelity calculation tools, but it also works for the traditional multi-stage sequence based on spatial homogenization.

The benchmark description can be summarized as follows:

- Very detailed geometry description of the initial core of a 1000 MWe Westinghouse PWR (193 fuel assemblies with 17×17 pin configuration)
- Three fuel enrichments: 1.6, 2.4 and 3.1 wt-% ^{235}U[a]
- Boron silicate glass burnable absorbers in five configurations: 6, 12, 15, 16 and 20 pins (9 different assembly types in total)
- Control rod bank worths and critical boron concentrations, as well as axial fission rate distribution at selected assembly positions provided for the initial HZP core
- Measured boron let-down curves provided for the first two operating cycles

[a] NOTE: This is an initial core, so all fuel assemblies start as fresh. The level of enrichment is consequently lower than for the typical equilibrium core (3-5 wt-% ^{235}U).

Example of spatial homogenization and core simulation

Example 1: MIT BEAVRS Benchmark with Serpent-ARES

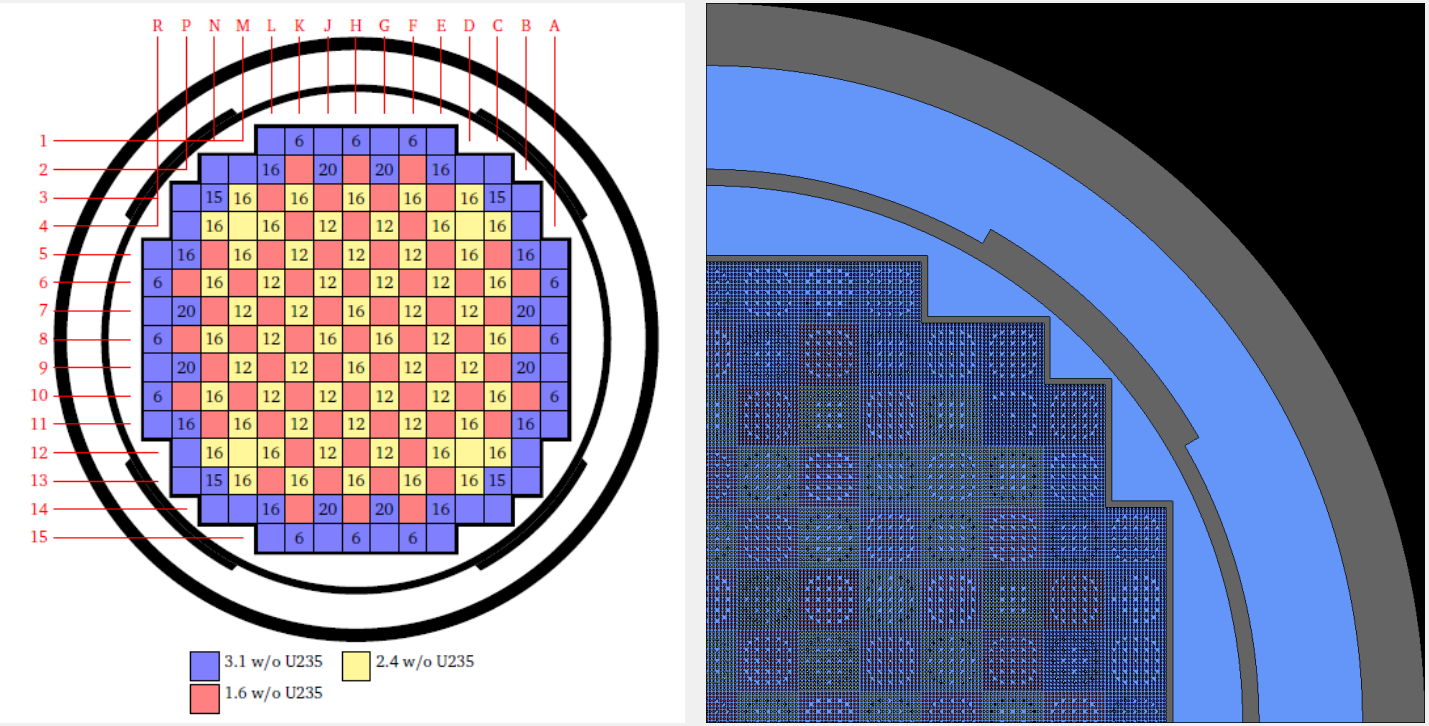

Figure 7 : Left: Layout of fuel assemblies showing fuel enrichment and positions of burnable absorbers (from BEAVRS benchmark specification available at the website). Right: Serpent geometry plot of a core quarter (reference 3D model).

Example of spatial homogenization and core simulation

Example 1: MIT BEAVRS Benchmark with Serpent-ARES

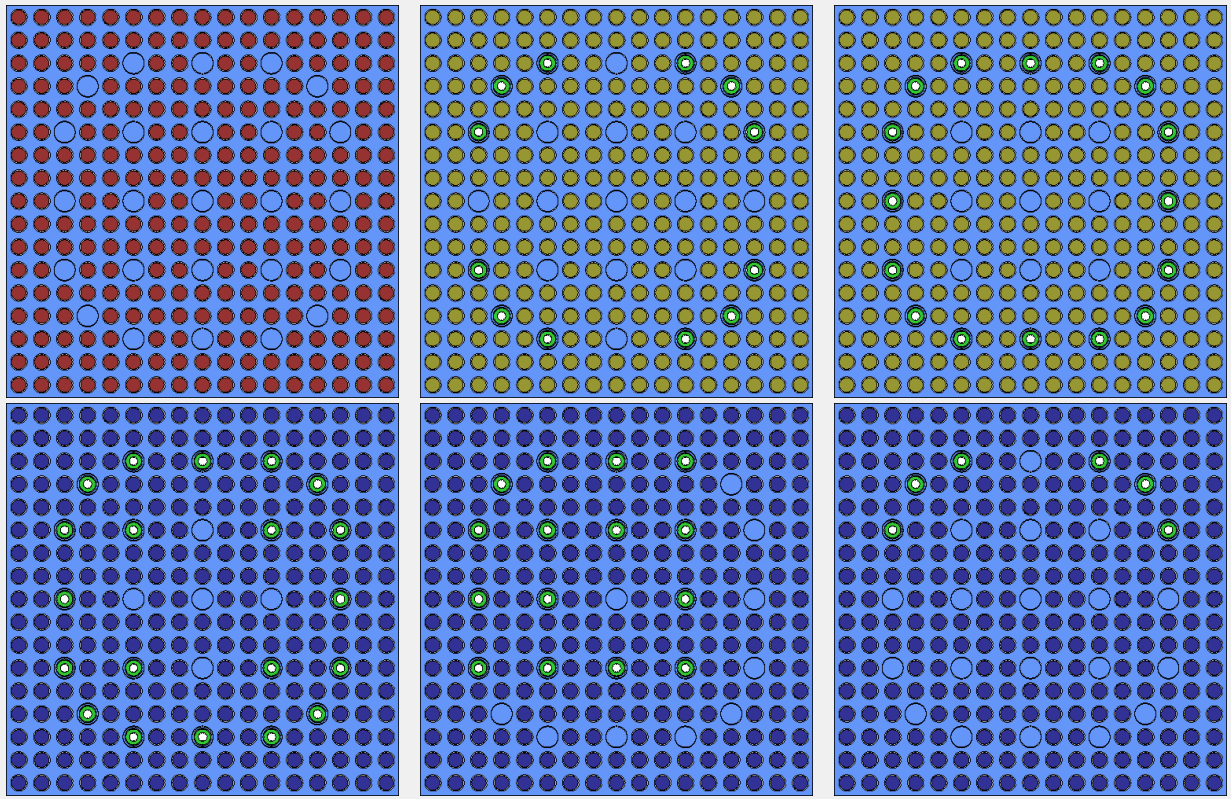

Figure 8 : Selected fuel assembly models used in spatial homogenization. Top row: 1.6 wt-% fuel, no BA, 2.4 wt-% fuel, 12 BA pins, 2.4 wt-% fuel, 16 BA pins. Bottom row: 3.1 wt-% fuel, 20 BA pins, 3.1 wt-% fuel, 15 BA pins, 3.1 wt-% fuel, 6 BA pins. Notice the asymmetric positioning of BA pins in the last two assemblies.

Example of spatial homogenization and core simulation

Example 1: MIT BEAVRS Benchmark with Serpent-ARES

The first part of the study involved HZP initial core calculation:

- All materials at uniform, pre-defined temperature
- Fixed boron concentration
- No reactivity feedbacks

Since there is no variation in the reactor operating conditions, group constant calculation had to be performed for a single state only. This is ideal for validating the neutronics model:

- No uncertainties from thermal hydraulics
- No additional errors from state-point or history parametrization
- Reference solution easily calculated with full-scale Monte Carlo simulation

In other words, if the calculation sequence works as is intended, it should reproduce the reference results. The remaining sources of error include:

- Approximations made in spatial homogenization (fuel assemblies separated from their actual surroundings)
- Validity of diffusion theory and the accuracy of the nodal diffusion model in ARES

Example of spatial homogenization and core simulation

Example 1: MIT BEAVRS Benchmark with Serpent-ARES

The approximations made in spatial homogenization turned out to be a major source of error in this particular case:

- The infinite lattice approximation failed completely for fuel assemblies locate at the core-reflector boundary, especially for the assembly type with asymmetrically positioned BA
- Modeling these assemblies with their immediate surroundings corrected the problem
- Getting the errors below 1% required homogenizing all assembly types in “colorset” configuration, which is not a practical solution when burnup is involved

Spatial detail included in the 3D reference model but omitted in the ARES calculation turned out to be surprisingly significant:

- Fuel spacers caused local dips in the axial power profile, which were not caught by the homogeneous model
- Gas-filled instrumentation tubes located at selected assembly positions had significant effect in the power level of surrounding fuel pins, and caused a noticeable global tilt in the radial power distribution

Even so, the results were found to be in good agreement. At core mid-plane, the errors in reconstructed pin-powers, for example, were below 1% in 82% of all fuel pins.

Example of spatial homogenization and core simulation

Example 1: MIT BEAVRS Benchmark with Serpent-ARES

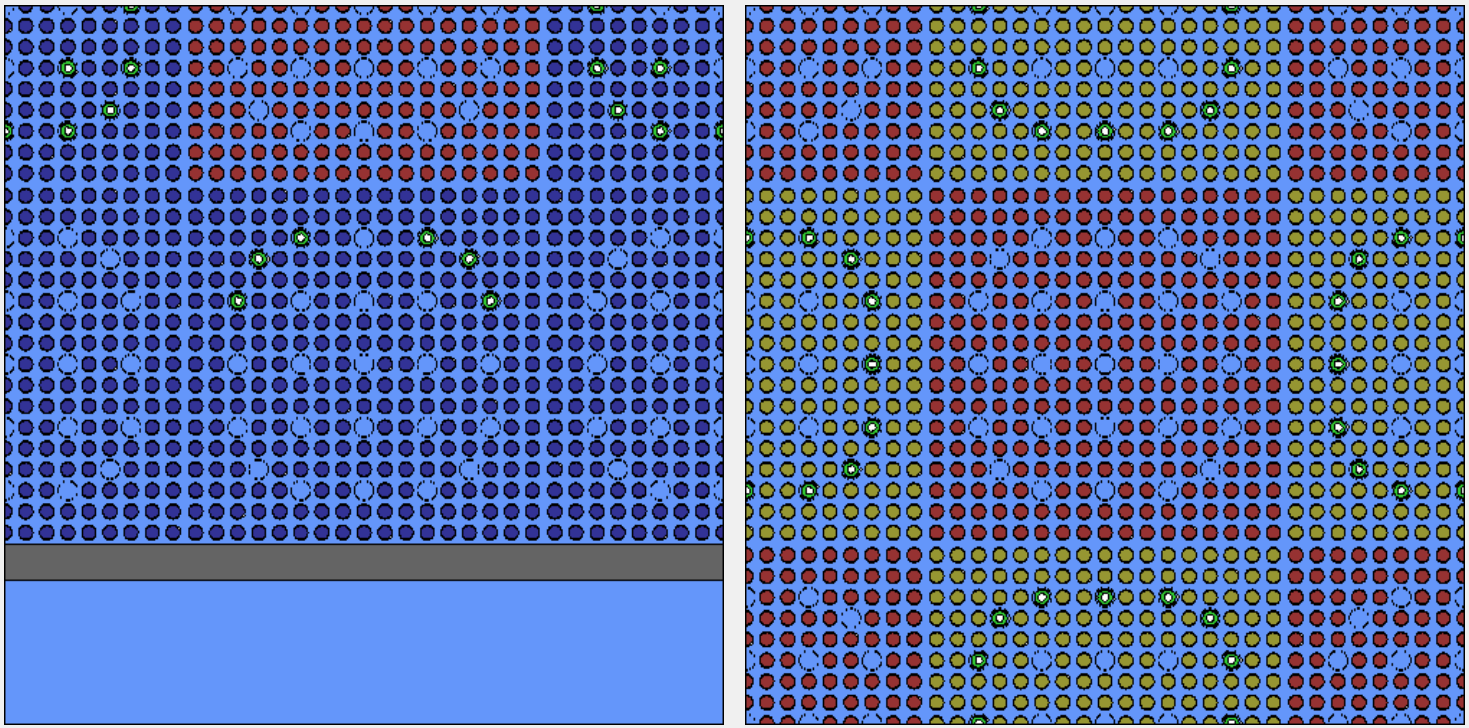

Figure 9 : Examples of geometries used in spatial homogenization when the immediate surroundings of the homogenized assembly were included. Left: 3.1 wt-% fuel assembly with 6 asymmetrically positioned burnable absorber pins at the core-reflector boundary. Right: 1.6 wt-% fuel assembly in a “colorset” configuration surrounded by 2.5 wt-% fuel.

Example of spatial homogenization and core simulation

Example 1: MIT BEAVRS Benchmark with Serpent-ARES

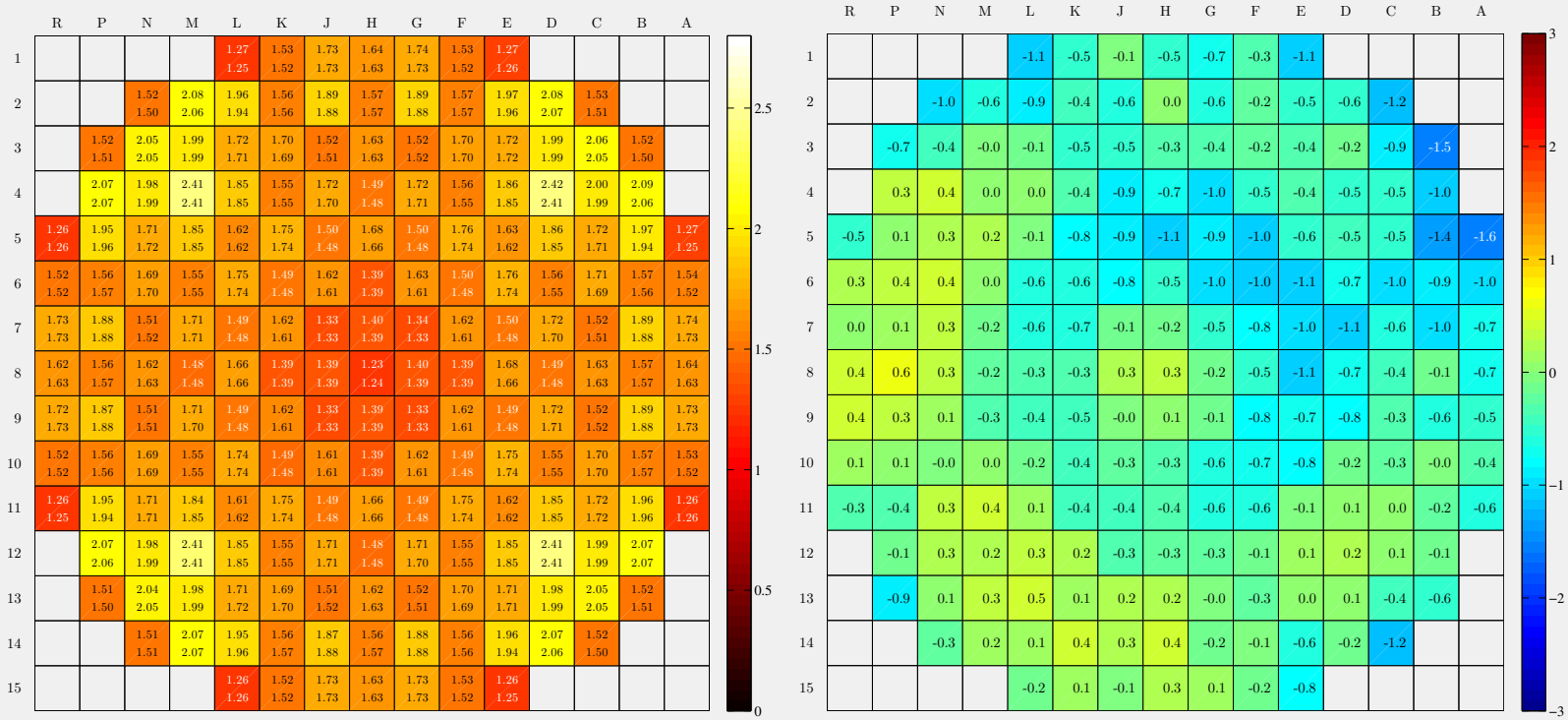

Figure 10 : Node-wise power distribution for the HZP core at core mid-plane. Left: results of Serpent-ARES and Serpent 3D reference calculation. Right: relative errors in percent. The 3D reference solution has a slight tilt in the South-West - North-East direction, caused by the asymmetric positioning of gas-filled instrumentation tubes. This effect is not caught by the homogeneous ARES model.

Example of spatial homogenization and core simulation

Example 1: MIT BEAVRS Benchmark with Serpent-ARES

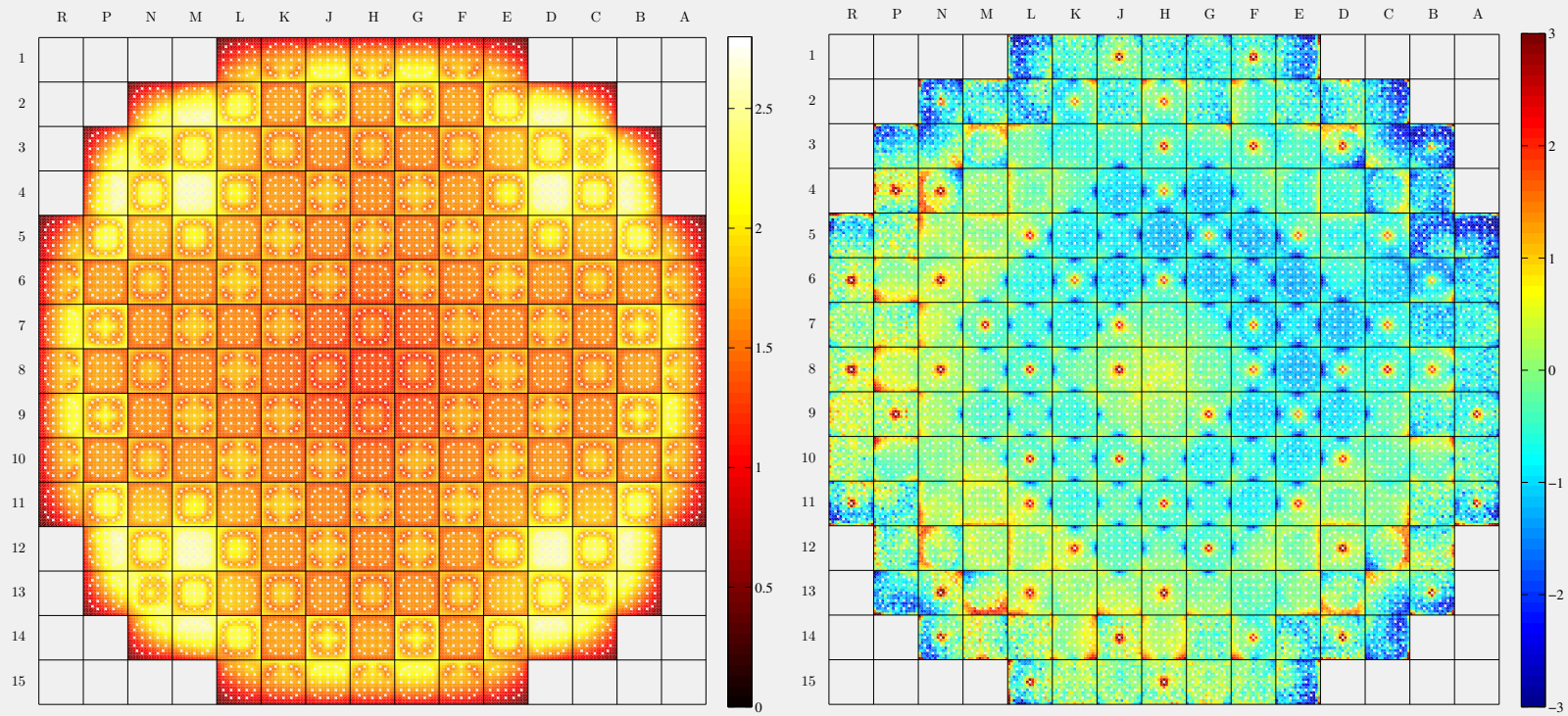

Figure 11 : Pin-wise power distribution for the HZP core at core mid-plane. Left: results of Serpent 3D reference calculation. Right: relative errors between the pin-power reconstruction and the reference 3D solution. The local effects of the gas-filled instrumentation tubes are clearly visible as red circles surrounding the central tube.

Example of spatial homogenization and core simulation

Example 1: MIT BEAVRS Benchmark with Serpent-ARES

The complete results of the first stage are published in Ann. Nucl. Energy.[a] The second stage involved calculation of control rod worths and critical boron concentrations for the HZP state and power distribution for the HFP state:

- Instead of a single pre-defined state point, the group constant data had to cover the range of temperatures and densities within the reactor core and variation in boron concentration
- Parametrization of group constants adds a new source of error and uncertainty
- The thermal hydraulics solution from ARES was used as part of the input in the Serpent 3D reference calculation
- No need for history variations because burnup calculation was not performed

Based on previous experience the core model was slightly simplified:

- The gas-filled instrumentation tubes were removed, which made the reference solution symmetrical and more consistent with the ARES model
- The geometry models used in spatial homogenization were simplified: only the outermost ring of assemblies were homogenized with their immediate surroundings

[a] J. Leppänen, R. Mattila and M. Pusa. "Validation of the Serpent-ARES code sequence using the MIT BEAVRS benchmark – Initial core at HZP conditions." Ann. Nucl. Energy, 69 (2014) 212-225.

Example of spatial homogenization and core simulation

Example 1: MIT BEAVRS Benchmark with Serpent-ARES

Table 1 : Critical boron concentrations for the HZP core (ppm).

Configuration	ARES	Ref.	Diff.
ARO	972	975	-3
D	910	902	8
C,D	812	810	2
A,B,C,D	677	686	-9
A,B,C,D,SE,SD,SC	488	508	-20

Table 2 : Control rod bank worths for the HZP core (pcm).

Rod bank	ARES	Ref.	Diff.
D	794	788	6
C	1232	1203	29
B	1206	1171	35
A	563	548	15
SE	473	461	12
SD	786	772	14
SC	1109	1099	10

Example of spatial homogenization and core simulation

Example 1: MIT BEAVRS Benchmark with Serpent-ARES

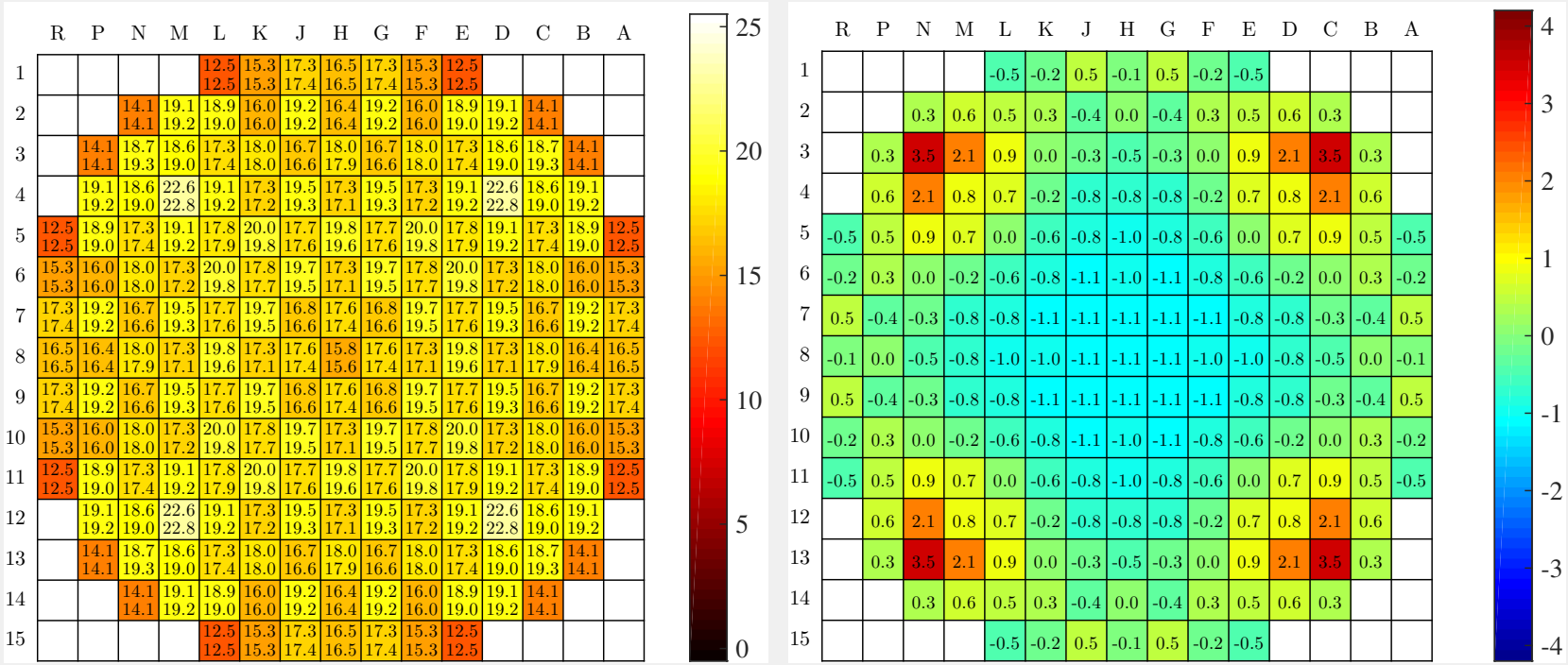

Figure 12 : Assembly powers for the HFP initial core. Left: results of Serpent-ARES and Serpent 3D reference calculation. Right: relative errors in percent. Fuel and coolant temperature and density distributions for the 3D Serpent reference solution were obtained from the ARES calculation.

Example of spatial homogenization and core simulation

Example 1: MIT BEAVRS Benchmark with Serpent-ARES

The final stage involved burnup simulation over the first reactor operating cycle. This required including history variations in group constant generation, which considerably increased the extent of the calculation task:

- A total of 81 burnup history calculations (9 assembly types, 3 coolant temperature histories: 566.5, 583.0 and 600.0K, 3 boron histories: 0, 350 and 700 ppm)
- Maximum of 42 state-point combinations in branch variations (fuel temperature: 600, 900 and 1200K, moderator temperature: 550, 575 and 600K, coolant void:[a] 0, 10 and 15%, control rods: withdrawn, inserted)
- Restarts at 15 burnup points between 0 and 50 MWd/kgU

The procedure involved repeating the Monte Carlo transport simulation more than 16000 times (including the burnup calculation with predictor-corrector steps and restarts performed for group constant generation)

The calculations were run VTT's computer cluster with 10 million neutron histories per transport simulation. The overall wall-clock running time was 46 hours, when multiple history cases were run simultaneously. The study is published in Ann. Nucl. Energy.[b]

[a] Accounts for sub-cooled boiling, variation in density is included in the temperature branches.

[b] Leppänen, J. and Mattila, R. ' 'Validation of the Serpent-ARES code sequence using the MIT BEAVRS benchmark – HFP conditions and fuel cycle 1 simulations." Ann. Nucl. Energy, 96 (2016) 324-331.

Example of spatial homogenization and core simulation

Example 1: MIT BEAVRS Benchmark with Serpent-ARES

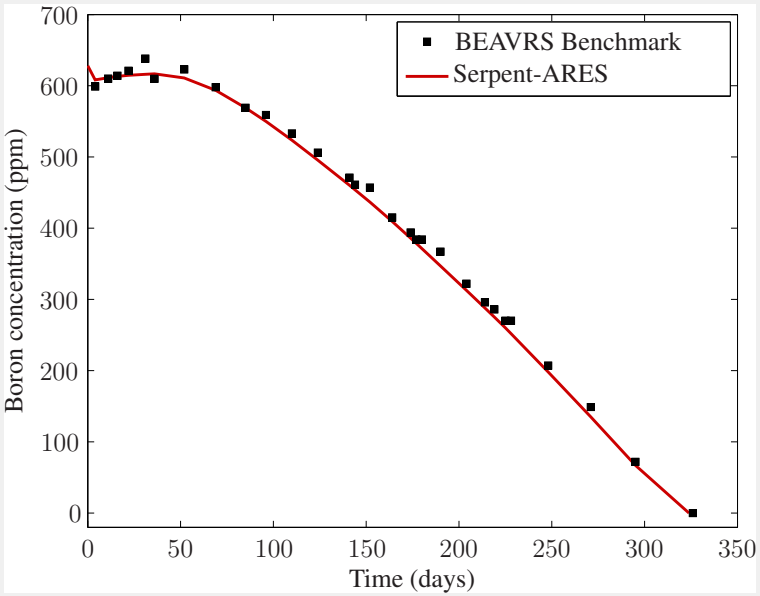

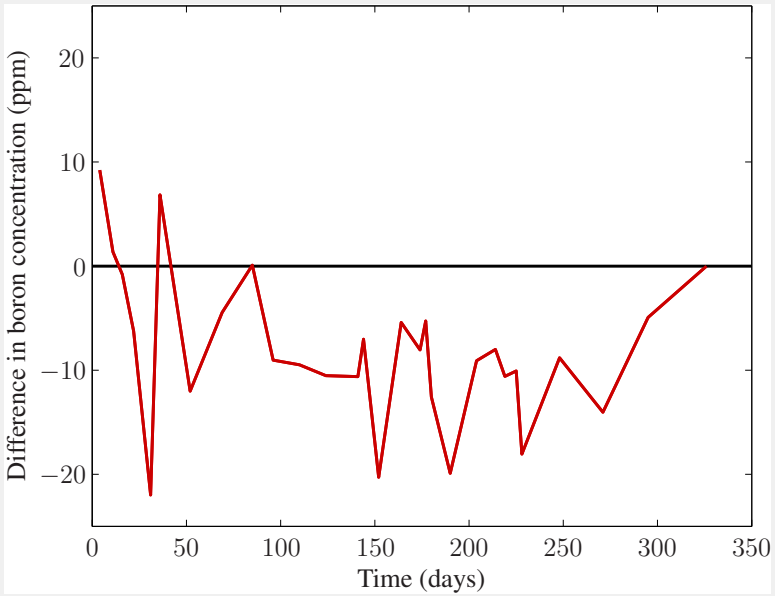

Figure 13 : Boron let-down curve calculated by Serpent-ARES compared to measured results provided in the benchmark specification.

Summary of main topics

This and the previous lecture covered the multi-stage calculation scheme applied in the modeling of operating nuclear reactors, for example, for the purpose of fuel cycle simulations and transient analysis. The computational task is divided in parts, and the complexity is gradually reduced while simultaneously moving towards larger spatial scale.

Full-core calculations are based on the solution of homogenized transport problem, which allows obtaining the solution at an acceptable computational cost for iterative thermal hydraulics coupling and simulation of core burnup. The validity of the scheme relies on the condensation of the complex interaction physics into a handful of homogenized few-group constants.

In state-of-the-art core simulators the global homogeneous flux solution is typically obtained using nodal diffusion methods, in which individual intra-nodal flux solutions are coupled together with continuity conditions and discontinuity factors. The heterogeneous flux solution can be recovered by pin-power reconstruction.

Since the dependence of interaction parameters on thermal hydraulic state and burnup is lost in the process of homogenization, the procedure is repeated in such way that all reactor operating conditions are covered. The few-group constants are parametrized, and the local values are obtained by interpolation.

The accuracy of nodal diffusion codes is considered sufficient for LWR design and safety studies, but the methodology has its limitations, which have to be taken into account. This requires some expertise from the code user.